Biochemical and Biophysical Research Communications 425 (2012) 333–339

Contents lists available at SciVerse ScienceDirect

Biochemical and Biophysical Research Communications

journal homepage: www.elsevier.com/locate/ybbrc

Quantitative multiplex quantum dot in-situ hybridisation based gene expression profiling in tissue microarrays identifies prognostic genes in acute myeloid leukaemia

Eleni Tholouli [a], Sarah MacDermott [b,1], Judith Hoyland [c], John Liu Yin [a], Richard Byers [d,*]

[a] Department of Haematology, Manchester Royal Infirmary, Oxford Road, Manchester, M13 9WL, UK
[b] The Medical School, The University of Manchester, Oxford Road, M13 9PT Manchester, UK
[c] School of Biomedicine, Faculty of Medical and Human Sciences, The University of Manchester, Oxford Road, M13 9PT Manchester, UK
[d] School of Cancer and Enabling Sciences, Faculty of Medical and Human Sciences, The University of Manchester, Stopford Building, Oxford Road, M13 9PT Manchester, UK

ARTICLE INFO

Article history:
Received 13 July 2012
Available online 25 July 2012

Keywords:
Quantum dots
Spectral imaging
Tissue microarrays
Acute myeloid leukaemia
Prognosis
Gene expression

ABSTRACT

Measurement and validation of microarray gene signatures in routine clinical samples is problematic and a rate limiting step in translational research. In order to facilitate measurement of microarray identified gene signatures in routine clinical tissue a novel method combining quantum dot based oligonucleotide *in situ* hybridisation (QD-ISH) and post-hybridisation spectral image analysis was used for multiplex *in-situ* transcript detection in archival bone marrow trephine samples from patients with acute myeloid leukaemia (AML). Tissue-microarrays were prepared into which white cell pellets were spiked as a standard. Tissue microarrays were made using routinely processed bone marrow trephines from 242 patients with AML. QD-ISH was performed for six candidate prognostic genes using triplex QD-ISH for *DNMT1, DNMT3A, DNMT3B,* and for *HOXA4, HOXA9, Meis1*. Scrambled oligonucleotides were used to correct for background staining followed by normalisation of expression against the expression values for the white cell pellet standard. Survival analysis demonstrated that low expression of *HOXA4* was associated with poorer overall survival ($p = 0.009$), whilst high expression of *HOXA9* ($p < 0.0001$), *Meis1* ($p = 0.005$) and *DNMT3A* ($p = 0.04$) were associated with early treatment failure. These results demonstrate application of a standardised, quantitative multiplex QD-ISH method for identification of prognostic markers in formalin-fixed paraffin-embedded clinical samples, facilitating measurement of gene expression signatures in routine clinical samples.

1. Introduction

Diagnosis of cancer typically relies on morphological appearances and immunohistochemistry (IHC), together, in some cancers, with cytogenetic and molecular analyses. However, in the emerging era of tailored therapy there is a growing need for new predictive biomarkers. Global gene expression profiling using microarrays has been used to identify such markers. However, though expression microarrays are ideal for discovery their use is limited by lack of morphological correlation, a semi-quantitative nature and requirement for high quality fresh-frozen tissues, most routinely processed biopsy samples being in the form of formalin-fixed and paraffin-embedded tissue (FFPET) [1]. A combined approach enabling quantitative measurement of the expression of multiple genes together with morphological assessment in fixed tissue samples would overcome the above problems and provide a tool for investigation of the expression patterns and roles of microarray identified genes in cancer.

In situ hybridisation (ISH) and IHC can be used for *in situ* visualisation of mRNA and protein, respectively in routinely processed FFPET sections [2]. Whilst IHC is limited by the availability of antibodies, probes for ISH can easily be constructed for any gene of interest [2,3]. However, ISH has been compromised by poor signal-to-noise ratio due to low fluorescence efficiency of fluorescent markers and high autofluorescence of paraffin embedded tissues [4–7]. Additionally, neither ISH nor IHC are quantitative in most studies.

We have previously demonstrated the utility of a novel quantum dot (QD) based ISH (QD-ISH) method in FFPET [8,9]. In order to facilitate translation of this approach to clinical research and diagnostics, this method requires capacity for high-throughput, and robust quantitation and standardisation to correct for inter-experimental and inter-laboratory variations. Jubb et al. [10] were the first to use standards for quantitative analysis of tumor markers identified by IHC and ISH in tissue microarrays (TMAs),

* Corresponding author. Address: Department of Histopathology, Manchester Royal Infirmary, Oxford Road, Manchester M13 9WL, UK. Fax: +44 161 276 6348.
E-mail address: richard.byers@cmft.nhs.uk (R. Byers).
[1] Present address: The Medical School, The University of Leeds, Leeds, UK.

0006-291X/$ - see front matter © 2012 Elsevier Inc. All rights reserved.
http://dx.doi.org/10.1016/j.bbrc.2012.07.092

embedding sense and anti-sense RNA standards into agarose. However, RNA strips do not fully recapitulate tissue as their hybridisation kinetics are likely to differ due to reasons of mRNA fixation in tissue and the presence of surface irregularity after tissue sectioning, both of which may result in different hybridisation efficiency. For this reason we used cell pellets embedded into agarose gel as standards across TMAs instead, the cellular nature of which more accurately reflects the hybridisation dynamics than does a synthetically prepared RNA sample. As previously described, we applied triplex QD-ISH and spectral imaging for data capture and analysis [9] and developed an equation for normalisation and standardisation of expression values. In the present study this method was applied to a large cohort of patients with acute myeloid leukaemia (AML), a genetically heterogeneous disease for which new prognostic molecular markers are needed.

Here we describe a novel method of quantitative expression measurement of multiple genes in routinely processed FFPET bone marrow trephines using multiplex QD-ISH in tissue microarrays, which allowed us to analyse a large number of patient samples.

2. Materials and methods

2.1. Sample selection

Presentation bone marrow trephine samples from 242 patients diagnosed with AML between 1994 and 2005 were retrieved from the histopathology archives at Manchester Royal Infirmary. All trephine biopsy samples were routinely processed, formalin-fixed, paraffin-embedded and EDTA decalcified at presentation. All material used was residual diagnostic tissue, anonymised and consent for its use in research granted.

2.2. Preparation of standard

For this, peripheral blood white cells were used. Thirty milliliters of peripheral blood was obtained prior to a peripheral blood haemopoietic progenitor cell collection. The donor had received 10 μg/kg granulocyte stimulating growth factor (Lenograstim; Chugai, London, UK) for 5 days prior to collection. Peripheral blood was poured into Ficoll (Pharmacia, St Albans, UK) and centrifuged at 2000 rpm for 20 min. The mononuclear layer was removed, washed with normal saline and fixed in 4% (v/v) formaldehyde/PBS (Genta Medical, York, UK). White cell pellets were then embedded in agar (Agar Scientific, Essex, UK) followed by embedding in paraffin wax using standard protocols.

2.3. TMA construction

Tissue microarrays were prepared using an ATA 100 tissue array machine (Chemicon International, Temecula, CA, USA). For this, cylindrical cores 1.5 mm in diameter were taken from paraffin embedded bone marrow trephine samples using a hollow needle and inserted into a precisely spaced 'recipient' paraffin wax block. Cores were obtained from areas showing leukaemic infiltration on H&E staining.

Each TMA contained between 20 and 24 different patient samples. From each patient sample three cores were removed and placed at different sites of the TMA block to maximise separation between related cores within a TMA. Similarly, three cores of the pre-prepared cell pellets were embedded in each TMA. A total of fourteen TMAs were prepared. Sections were cut from the TMA blocks and mounted onto coated glass slides; using four micron thick sections for H&E staining and seven micron sections for ISH. Each core from each patient contained at least 20% leukaemic blasts and was representative of the whole trephine sample.

2.4. In situ hybridisation

A total of six genes from two gene families were studied: *HOXA4*, *HOXA9* and *Meis1* from the homeobox gene family, and *DNMT1, DNMT3A* and *DNMT3B* from the DNA-methyl transferases. ABL and beta 2 microglobulin were used as housekeeping genes to evaluate sample viability; ABL is a well established housekeeping gene and used widely in gene expression analysis in acute leukaemia. Anti-sense cDNA oligonucleotide probe sequences (50-mer) specific to the above genes and their corresponding scramble probes were used (anti-sense probe sequences are shown in Table 1). The probes were HPLC purified and biotin modified via a TEG spacer at the 3′end (Eurogentec, Seraing, Belgium). Probes targeting the genes from each gene family were conjugated to three different quantum dots (QDs) (605, 655, 705 nm) per family. Triplex QD-ISH for each family was performed on 7 μm thick sections for both anti-sense and scramble probes. QD-ISH for the control genes was performed in duplex. Probe design and QD-ISH was performed as previously detailed in Tholouli et al. [9].

2.5. Imaging analysis

Up to four images per core sample were captured at 400× using a Leitz Diaplan fluorescence microscope (Leitz, Germany) with a 490 nm excitation long pass filter and a CRI Nuance spectral analyzer (Cambridge Research and Instrumentation Inc., Woburn, USA) [9]. Images were collected using a standard exposure time of 1000 ms at 5 nm wavelength intervals from 450 to 720 nm creating a 3D optical profile (cube) with the dimensions *x*, *y* and wavelength, containing the complete spectral information for every pixel at each wavelength. Using the spectra for autofluorescence and that of the relevant QDs, spectral unmixing allowed digital separation of this information [11].

2.6. Signal quantitation

The resultant unmixed images were then transferred to IPLab (Scanalytics, MD, USA) for measurement of fluorescent signal

Table 1
Reverse complement sequences of anti-sense probes.

Gene	Reverse complement oligonucleotide sequence
ABL	5′-ACTCAGACCCTGAGGCTCAAAGTCAGATGCTACTGGCCGCTGAAGGGCTT-3′
β2M	5′-CCAGAAAGAGAGAGTAGCGCGAGCACAGCTAAGGCCACGGAGCGAGACAT-3′
HOXA9	5′-CCGCTTTTTCCGAGTGGAGCGCGCATGAAGCCAGTTGGCTGCTGGGTTAT-3′
HOXA4	5′-CTCGAAGGGAGGGAACTTGGGCTCGATGTAGTTGGAGTTTATCAAAAACG-3′
Meis1	5′-CCTCCATGCCCATATTCATGCCCATTCCACTCATAGGTCCTGGTGCTCTA-3′
DNMT1	5′-GCCAGGTAGCCCTCCTCGGATAATTCTTCTTTACGTAATTTGGTTTCCAA-3′
DNMT3A	5′-TTCTCAACACACACCACTGAGAATTTGCCGTCTCCGAACCACATGACCCA-3′
DNMT3B	5′-AGTTTGTCTGCAGAGACCTCGGAGAACTTGCCATCGCCAAACCACTGGAC-3′

β2 M = β2 microglobulin.

intensity of each gene in each sample. For the cell pellets, each white cell was individually marked and fluorescence measured. The resulting data was transferred to Excel (Microsoft Office, Seattle, USA) and the mean calculated using all 3 cores of each sample for each gene. For the cell pellets, the average numerical value across all cells and all cores for each TMA was calculated.

2.7. Statistical analysis

The mean expression of each gene was calculated for each patient, divided into quartiles and correlated with clinical outcome data. Statistical analysis was performed using the chi-square test on contingency tables and Mann Whitney-*U*. Overall survival (OS) and disease free survival (DFS) were analysed using Kaplan–Meier analysis and Cox regression was performed for univariate and multivariate analysis.

3. Results

3.1. Patients

Clinical data including patient age, diagnostic information, treatment, remission status and survival details were collected for all 242 patients. For statistical analysis, 192 AML patients were included as the remainder either died before, during or immediately after one course of chemotherapy or incomplete data was available. The median age in these patients was 52 years (range 17–77) with an equal proportion of males to females. Patient demographics are summarised in Table 2. All patients included received intensive chemotherapy according to standard UK MRC AML protocols.

Table 2
Patient demographics (n = 192).

Median age (range)	52 years (17–77)	$P < 0.0001$
<60 years	134	
⩾60 years	58	
Sex		
Female	97	$P = 0.143$
Male	95	
WCC at diagnosis		
$<100 \times 10^9$/L	176	$P = 0.009$
$\geqslant 100 \times 10^9$/L	16	
AML		
De Novo	163	$P = 0.056$
Secondary	29	
FAB classification		
M0	13	$P = 0.008$
M1	47	
M2	49	
M3	17	
M4	18	
M5	13	
M6	13	
M7	7	
Not available	15	
Cytogenetics		
Good	29	$P < 0.0001$
Intermediate	108	
Poor	26	
Not evaluated	29	
Disease status post induction chemotherapy		
Complete remission (<5% blasts)	147	$P < 0.0001$
Partial remission (5–14.9% blasts)	9	
Residual disease (⩾15% blasts)	36	
Stem cell transplant	66	
Autologous	15	$P < 0.0001$
Allogeneic sibling/unrelated donor	51	

3.2. Method standardization and quality control

To correct for inter-experimental variability peripheral blood white cell pellets embedded in agar were used as a standard across each TMA. Composition of these cell pellets was defined using a manual differential cell count on haematoxylin and eosin (H&E) stained sections demonstrating a uniform myeloid to lymphoid ratio of approximately 1:5 across all TMAs and including a mixture of myeloid cells from immature progenitors (myeloblasts) to mature neutrophils. Viability of sample mRNA was evaluated by measurement of expression of the housekeeping genes *ABL* and beta 2 microglobulin which were present in all cores.

3.3. Gene expression measurement

Triplex QD-ISH was successfully performed for all genes and hybridisation signal intensity measured for each gene in each sample (Fig. 1a and b). The signal intensity values were corrected for background staining and normalised to the standards (Fig. 2a and b) and as detailed below (the resultant equation is shown in Fig. 2c). First, signal intensity was measured in patient samples for both anti-sense and scrambled probes for each core. Next, the signal intensity of all three representative cores, anti-sense and scramble, was used to calculate the mean anti-sense and scramble

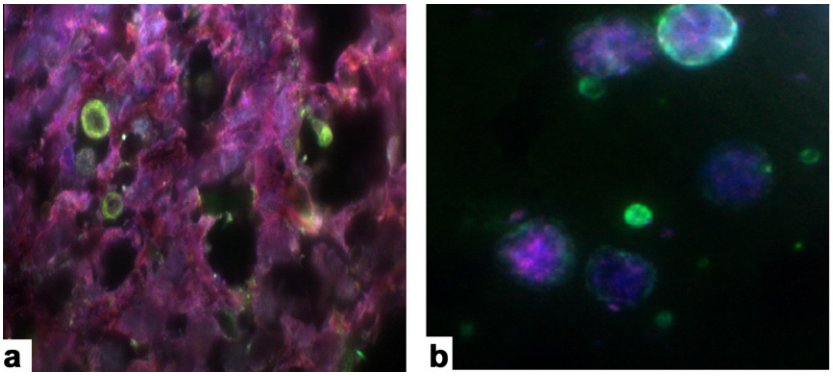

Fig. 1. Composite images following triplex QD-ISH. (a) TMA core of a patient sample with AML following triplex QD-ISH using anti-sense probes for *DNMT3A, DNMT1* and *DNMT3B* (×1000). Hybridisation signal displayed for *DNMT3A* was pseudo-colored red, for *DNMT1* was pseudo-colored green and for *DNMT3B* was pseudo-colored blue. (b) TMA core of white cell pellet standard following triplex QD-ISH using anti-sense probes for *HOXA4, Meis1* and *HOXA9* (×1000). Hybridisation signal displayed for *HOXA4* was pseudo-colored red, for *Meis1* was pseudo-colored green and for *HOXA9* was pseudo-colored blue(For interpretation of the references to colour in this figure legend, the reader is referred to the web version of this article.).

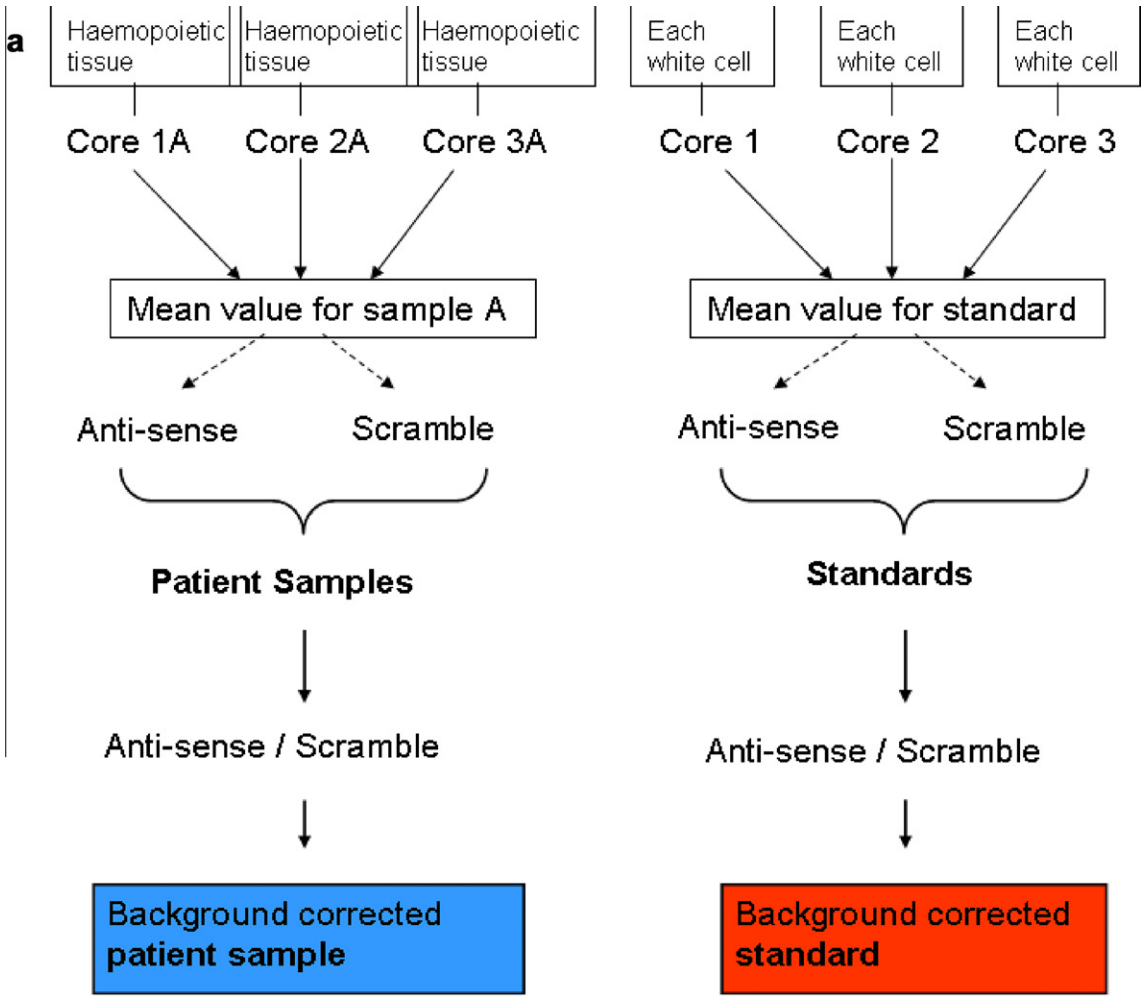

c

$$Y_x = \frac{M(x_1 + x_2 + x_3) / M_s(x_{s1} + x_{s2} + x_{s3})}{M(n_1 + n_2 + n_3) / M_s(n_{s1} + n_{s2} + n_{s3})}$$

Fig. 2. Flow chart for calculation of standardisation and normalisation of gene expression values. (a) The mean intensity for each sample and standard was measured and calculated for all three cores for both anti-sense and scramble before division for background correction. (b) Background corrected patient samples were then divided by the background corrected standard for that TMA for that gene. (c) Equation. *Yx* = normalized and standardized value for sample x; *M* = mean anti-sense value; *Ms* = mean scramble value; x1-3 = measurements of anti-sense values for sample x from cores 1-3; xs1-3 = measurement of scramble value for sample x from cores 1-3; n1-3 = measurements for anti-sense values for standards 1-3; ns1-3 = measurement for scramble values for standards 1-3.

signal intensities for each sample. The mean anti-sense intensity value for each patient sample was then corrected for background hybridisation signal by division by the mean scramble signal for that sample. This allowed for correction of anti-sense probe intensity against background noise; this principle is used for background noise correction in microarray studies. The same procedure was performed for the standards with the exception that signal intensity was measured in each white cell in each core. Finally, the background corrected anti-sense signal intensity for each patient sample was normalised by division by the background

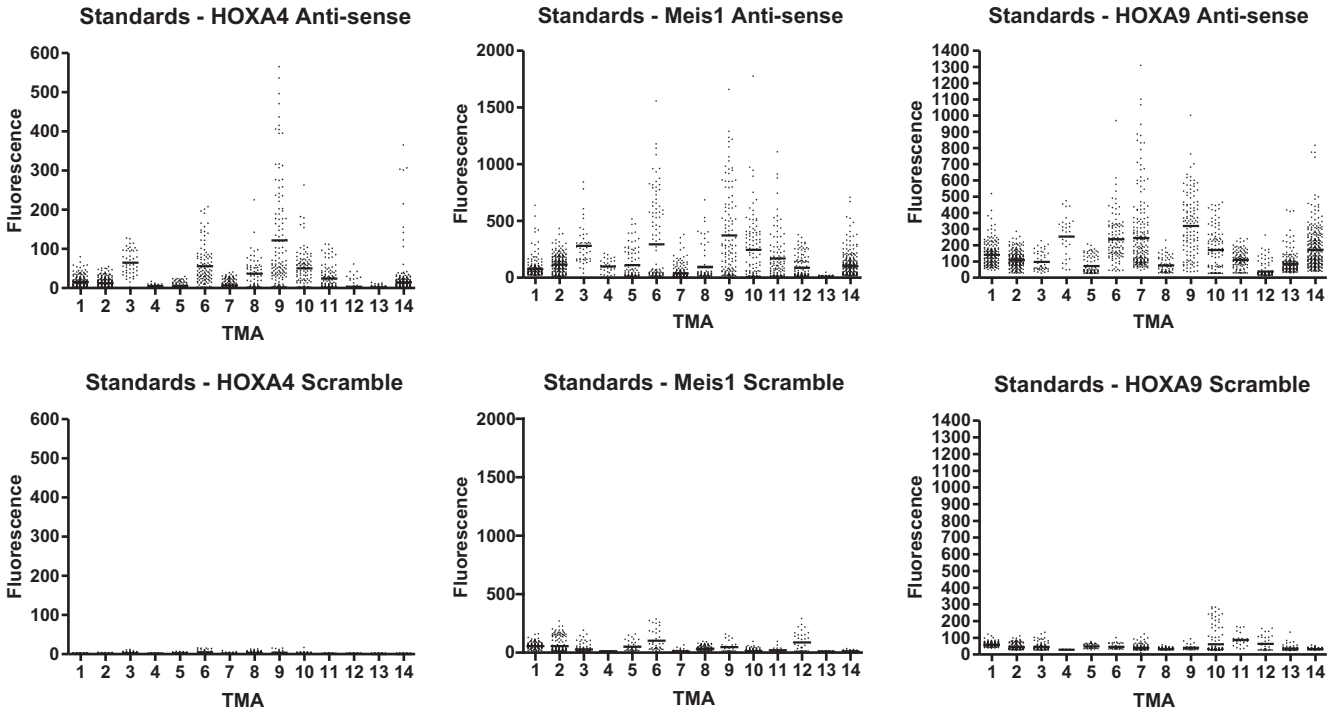

Fig. 3. Hybridisation signal intensity of white cell pellet standards in each TMA for *HOXA4, HOXA9* and *Meis1*. Fluorescence intensity is displayed for each cell in each pellet in each TMA (each dot in histogram corresponds to single cell signal intensity, mean for each TMA displayed as horizontal bar), demonstrating marked variation of signal expression values for the standards across all TMAs; anti-sense intensity values shown for representative genes (*HOXA4, Meis1* and *HOXA9*) in top panel and corresponding scramble intensity values shown in bottom panel, demonstrating low level background signal. Fluorescence intensity is displayed in arbitrary units.

corrected standard for the corresponding TMA. Normalisation against standards was required due to the presence of variability of un-normalised signal intensity values across the TMAs (Fig. 3).

3.4. Survival analysis

The overall survival in this cohort of patients was 43% at 5 years. Older age ($\geqslant$60 years), high white blood count at diagnosis ($\geqslant 100 \times 10^9$/L) and adverse cytogenetics were associated with poorer outcome. In addition, achieving CR was an independent prognostic marker for survival (Fig. 4a).

Low *HOXA4* expression (median 577; [95% CI 325–828]) was associated with poorer OS ($p = 0.013$) by Kaplan-Meier analysis (Fig. 4b) and disease free survival (DFS) ($p = 0.025$) by Cox regression. High expression of *HOXA9* (median 0.843 [0.145–7.479]; $p < 0.0001$), *Meis1* (median 0.716 [0.05–7.84]; $p = 0.005$) and *DNMT3A* (median 1.305 [0.073–5.477]; $p = 0.04$) were associated with failure to achieve CR (Fig. 4c–e). These, however, had no impact on OS or DFS. Expression levels of the remaining 5 genes did not show any association with CR, DFS or OS.

4. Discussion

Expression microarrays have identified prognostic and diagnostic biomarkers for an ever increasing number of cancers, and there is now a need to develop high-throughput analytical systems for validation of the hypotheses suggested by microarray results [12–14]. Furthermore, it is also desirable to correlate these markers with tissue morphology. We have sought to achieve this by using a novel method of multiplexed QD-ISH, which enables detection and measurement of several genes simultaneously. Additionally, to facilitate analysis of a large number of samples we have applied this method to TMAs representing 242 cases of AML.

The standardised normalised expression values *HOXA4*, *HOXA9*, *DNMT3A* and *Meis1* were associated with outcome. Specifically, concordant with other reports, low expression of *HOXA4* was associated with poor outcome in adult AML [15]. Similarly, in the present study high levels of *HOXA9* and *Meis1* were associated with treatment failure, as previously demonstrated by others [16–19]. Co-expression of *Meis1* with *HOXA9* has been shown to be leukaemogenic in both murine and human AML [18,20], and though AML may be induced by over-expression of either gene alone the process was accelerated by their co-expression [18,20,21] with or without the presence of any fusion genes such as *nucleoporin (NUP)98/HOXA9* [22]. These transcription factors of the homeobox gene family are believed to control cytokine-specific differentiation responses and are down-regulated during normal myelopoiesis [23]. In particular, they immortalise myeloid progenitors, prevent differentiation stimulated by G-CSF or GM-CSF and permit proliferation in response to stem cell factor. Meis1 over-expression may also induce apoptosis via a caspase-dependant mechanism which can be inhibited by proteins such as XIAP [24,25].

Using cDNA microarrays, Bullinger et al. [13] identified new molecular subtypes of AML, including two prognostically relevant subgroups in patients with normal karyotype, one of which showed a high expression of the methyltransferases *DNMT3A* and *DNMT3B* suggesting their potential role in leukaemic pathogenesis. This is consistent with previous studies which implicated aberrant hypermethylation of tumor suppressor genes in the development of many tumours, including hematological malignancies [26,27]. It is also thought that DNA methylation plays a role in control of the *p53* network. Esteve et al. [28] demonstrated interaction between *DNMT1* and *p53* and showed that methylation of the *survivin* promotor region contributed to gene repression. Of the three DNMTs studied in this project, only *DNMT3A* was associated with treatment failure; association of *DNMT3A* with outcome has very recently been reported by Ley et al. who showed association of *DNMT3A* mutations with poor outcome in AML [29].

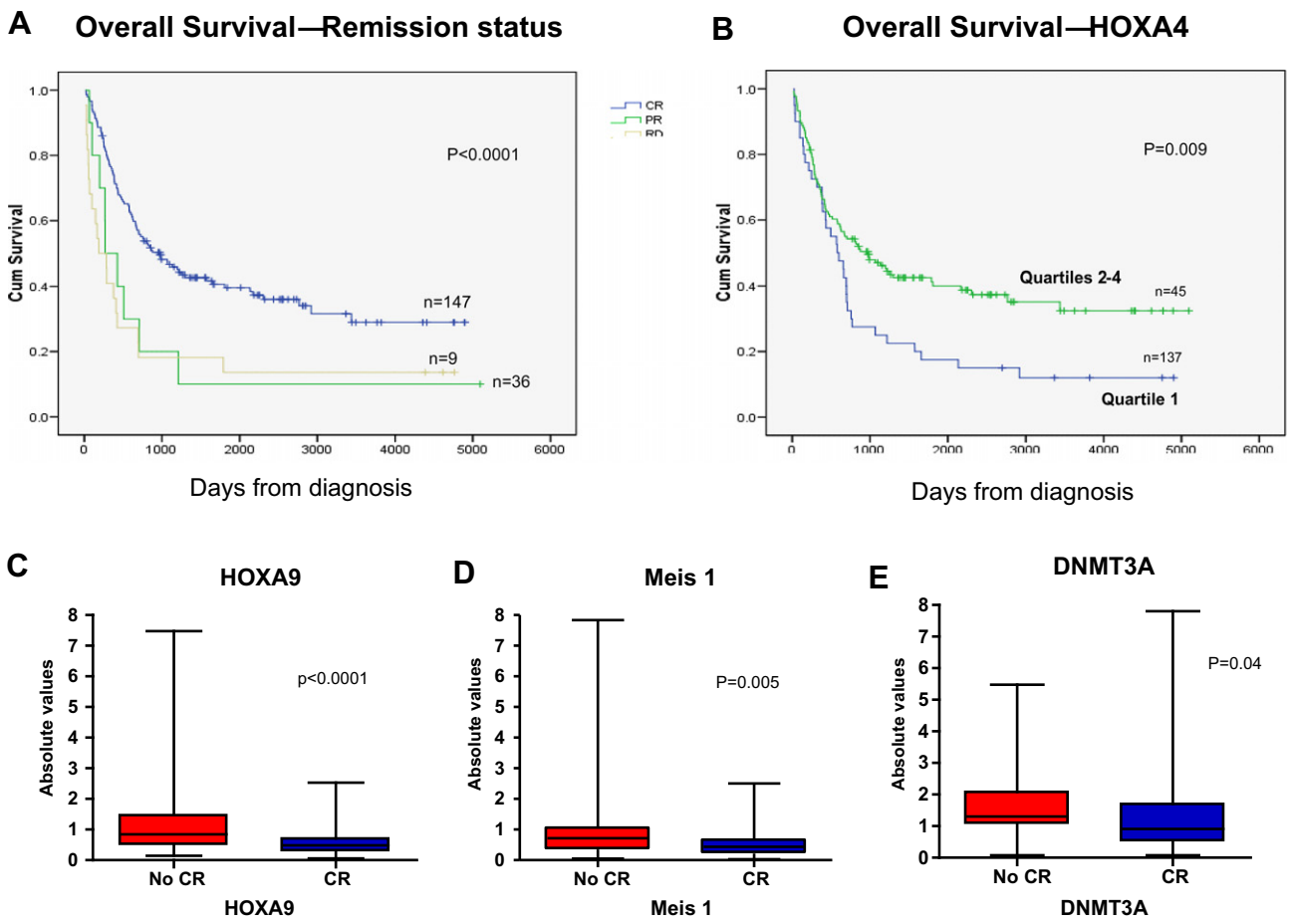

Fig. 4. Kaplan-Meier survival analysis of AML patients showed; (a) response to induction chemotherapy, specifically complete or partial remission, or refractory disease was predictive of overall survival, and that (b) low expression of HOXA4 was associated with poorer overall survival. High expression of HOXA9 (c), Meis1 (d) and DNMT3A (e) were associated with failure to achieve complete remission after induction chemotherapy.

Central to the new method developed is standardisation and normalisation of the expression data, which is key for direct comparison and reproducibility of quantitative *in situ* data, and which remains a significant challenge for both IHC and ISH. Jubb et al. addressed this by design of standards for quantitative ISH analysis of tumor markers [10]. They prepared TMAs using positive and negative control blocks containing synthetically prepared sense and anti-sense RNA strips which were embedded into agarose gel. Using Alexa fluorophores as well as radiolabelled riboprobes and a laser imaging system they quantitated expression of several genes and proteins in triplicates of colorectal tissues. In adapting our previously reported method of multiplex QD-ISH [9] for quantitative measurement in a TMA we instead used a cell pellet standard spiked in each TMA from which to normalise gene expression values. The approach taken described here is logistically simpler since white cell pellets are easily obtained and the cellular nature of such a standard more accurately reflects the hybridisation dynamics than does a synthetically prepared RNA pellet. Each white cell pellet was embedded into agarose gel, FFPE treated, and used for signal value normalisation, enabling quantitative comparison of data across multiple TMAs.

In summary, these results demonstrate application of standardised quantitative multiplex QD-ISH for identification of prognostic markers in FFPET samples. Low expression of *HOXA4* was associated with poor survival whilst high expression of *HOXA9, Meis1* and *DNMT3A* were linked to failure to achieve complete remission (CR). Furthermore application of the method to TMAs allows high sample throughput, use of archived materials and ease of transfer to a wide range of malignancies.

Acknowledgments

We would like to thank Caroline Glennie at the Department of Histopathology, Manchester Royal Infirmary, for performing all H&E stains for this study. We are grateful to Ric Swindell, The Christie, for statistical advice. We would also like to thank Crispin Miller, Head of Bioinformatics at the Paterson Institute for Cancer Research, Manchester, for his valuable contributions during discussions of data analysis and processing.

Author contributions: Eleni Tholouli – Performed experiments, data analysis and manuscript prepartation; Sarah MacDermott – Performed experiments and manuscript preparation; Judith A Hoyland – Design of experiments and manuscript preparation; John A Liu Yin – Design of experiments and manuscript preparation; Richard J Byers – Design of experiments and manuscript preparation.

References

[1] B.L. Ebert, T.R. Golub, Genomic approaches to hematologic malignancies, Blood 104 (2004) 923–932.

[2] J.N. Wilcox, Fundamental principles of in situ hybridization, J. Histochem. Cytochem. 41 (1993) 1725–1733.

[3] C.N. Kind, The application of in-situ hybridisation and immuno-cytochemistry to problem resolution in drug development, Toxicol. Lett. 112–113 (2000) 487–492.

[4] R.W. Dirks, R.P. Van Gijlswijk, M.A. Vooijs, A.B. Smit, J. Bogerd, J. van Minnen, A.K. Raap, M. Van der Ploeg, 3′-end fluorochromized and haptenized oligonucleotides as in situ hybridization probes for multiple, simultaneous RNA detection, Exp. Cell Res. 194 (1991) 310–315.
[5] P. Dittrich, F. Malvezzi-Campeggi, M. Jahnz, P. Schwille, Accessing molecular dynamics in cells by fluorescence correlation spectroscopy, Biol. Chem. 382 (2001) 491–494.
[6] B. Banerjee, B. Miedema, H.R. Chandrasekhar, Emission spectra of colonic tissue and endogenous fluorophores, Am. J. Med. Sci. 316 (1998) 220–226.
[7] P. Del Castillo, A.R. Llorente, J.C. Stockert, Influence of fixation, exciting light and section thickness on the primary fluorescence of samples for microfluorometric analysis, Basic Appl. Histochem. 33 (1989) 251–257.
[8] R.J. Byers, D. Di Vizio, F. O'Connell, E. Tholouli, R.M. Levenson, K. Gossage, D. Twomey, Y. Yang, E. Benedettini, J. Rose, K.L. Ligon, S.P. Finn, T.R. Golub, M. Loda, Semiautomated multiplexed quantum dot-based in situ hybridization and spectral deconvolution, J. Mol. Diagn. 9 (2007) 20–29.
[9] E. Tholouli, J.A. Hoyland, D. Di Vizio, F. O'Connell, S.A. Macdermott, D. Twomey, R. Levenson, J.A. Yin, T.R. Golub, M. Loda, R. Byers, Imaging of multiple mRNA targets using quantum dot based in situ hybridization and spectral deconvolution in clinical biopsies, Biochem. Biophys. Res. Commun. 348 (2006) 628–636.
[10] S. Jubb, T.H. Landon, J. Burwick, T.Q. Pham, G.D. Frantz, B. Cairns, P. Quirke, F.V. Peale, K.J. Hillan, Quantitative analysis of colorectal tissue microarrays by immunofluorescence and in situ hybridization, J. Pathol. 200 (2003) 577–588.
[11] D.L. Farkas, C. Du, G.W. Fisher, C. Lau, W. Niu, E.S. Wachman, R.M. Levenson, Non-invasive image acquisition and advanced processing in optical bioimaging, Comput. Med. Imaging Graph 22 (1998) 89–102.
[12] L. Bullinger, K. Dohner, E. Bair, S. Frohling, R.F. Schlenk, R. Tibshirani, H. Dohner, J.R. Pollack, Use of gene-expression profiling to identify prognostic subclasses in adult acute myeloid leukemia, N. Engl. J. Med. 350 (2004) 1605–1616.
[13] L. Bullinger, F.G. Rucker, S. Kurz, J. Du, C. Scholl, S. Sander, A. Corbacioglu, C. Lottaz, J. Krauter, S. Frohling, A. Ganser, R.F. Schlenk, K. Dohner, J.R. Pollack, H. Dohner, Gene-expression profiling identifies distinct subclasses of core binding factor acute myeloid leukemia, Blood 110 (2007) 1291–1300.
[14] P.J. Valk, R.G. Verhaak, M.A. Beijen, C.A. Erpelinck, S. Barjesteh van Waalwijk van Doorn-Khosrovani, J.M. Boer, H.B. Beverloo, M.J. Moorhouse, P.J. van der Spek, B. Lowenberg, and R. Delwel, Prognostically useful gene-expression profiles in acute myeloid leukemia. N. Engl. J. Med. 350 (2004) 1617–28.
[15] L. Grubach, C. Juhl-Christensen, A. Rethmeier, L.H. Olesen, A. Aggerholm, P. Hokland, M. Ostergaard, Gene expression profiling of Polycomb, Hox and Meis genes in patients with acute myeloid leukaemia, Eur. J. Haematol. 81 (2008) 112–122.
[16] T.R. Golub, D.K. Slonim, P. Tamayo, C. Huard, M. Gaasenbeek, J.P. Mesirov, H. Coller, M.L. Loh, J.R. Downing, M.A. Caligiuri, C.D. Bloomfield, E.S. Lander, Molecular classification of cancer: class discovery and class prediction by gene expression monitoring, Science 286 (1999) 531–537.
[17] H.A. Drabkin, C. Parsy, K. Ferguson, F. Guilhot, L. Lacotte, L. Roy, C. Zeng, A. Baron, S.P. Hunger, M. Varella-Garcia, R. Gemmill, F. Brizard, A. Brizard, J. Roche, Quantitative HOX expression in chromosomally defined subsets of acute myelogenous leukemia, Leukemia 16 (2002) 186–195.
[18] E. Kroon, J. Krosl, U. Thorsteinsdottir, S. Baban, A.M. Buchberg, G. Sauvageau, Hoxa9 transforms primary bone marrow cells through specific collaboration with Meis1a but not Pbx1b, Embo J. 17 (1998) 3714–3725.
[19] C.S. Wilson, G.S. Davidson, S.B. Martin, E. Andries, J. Potter, R. Harvey, K. Ar, Y. Xu, K.J. Kopecky, D.P. Ankerst, H. Gundacker, M.L. Slovak, M. Mosquera-Caro, I.M. Chen, D.L. Stirewalt, M. Murphy, F.A. Schultz, H. Kang, X. Wang, J.P. Radich, F.R. Appelbaum, S.R. Atlas, J. Godwin, C.L. Willman, Gene expression profiling of adult acute myeloid leukemia identifies novel biologic clusters for risk classification and outcome prediction, Blood 108 (2006) 685–696.
[20] U. Thorsteinsdottir, E. Kroon, L. Jerome, F. Blasi, G. Sauvageau, Defining roles for HOX and MEIS1 genes in induction of acute myeloid leukemia, Mol. Cell Biol. 21 (2001) 224–234.
[21] U. Thorsteinsdottir, A. Mamo, E. Kroon, L. Jerome, J. Bijl, H.J. Lawrence, K. Humphries, G. Sauvageau, Overexpression of the myeloid leukemia-associated Hoxa9 gene in bone marrow cells induces stem cell expansion, Blood 99 (2002) 121–129.
[22] K.R. Calvo, D.B. Sykes, M.P. Pasillas, M.P. Kamps, Nup98-HoxA9 immortalizes myeloid progenitors, enforces expression of Hoxa9, Hoxa7 and Meis1, and alters cytokine-specific responses in a manner similar to that induced by retroviral co-expression of Hoxa9 and Meis1, Oncogene 21 (2002) 4247–4256.
[23] K.R. Calvo, P.S. Knoepfler, D.B. Sykes, M.P. Pasillas, M.P. Kamps, Meis1a suppresses differentiation by G-CSF and promotes proliferation by SCF: potential mechanisms of cooperativity with Hoxa9 in myeloid leukemia, Proc. Natl. Acad. Sci. USA 98 (2001) 13120–13125.
[24] Q.L. Deveraux, N. Roy, H.R. Stennicke, T. Van Arsdale, Q. Zhou, S.M. Srinivasula, E.S. Alnemri, G.S. Salvesen, J.C. Reed, IAPs block apoptotic events induced by caspase-8 and cytochrome c by direct inhibition of distinct caspases, Embo J. 17 (1998) 2215–2223.
[25] P.J. Wermuth, A.M. Buchberg, Meis1-mediated apoptosis is caspase dependent and can be suppressed by coexpression of HoxA9 in murine and human cell lines, Blood 105 (2005) 1222–1230.
[26] K.D. Robertson, E. Uzvolgyi, G. Liang, C. Talmadge, J. Sumegi, F.A. Gonzales, P.A. Jones, The human DNA methyltransferases (DNMTs) 1, 3a and 3b: coordinate mRNA expression in normal tissues and overexpression in tumors, Nucleic Acids Res. 27 (1999) 2291–2298.
[27] S. Mizuno, T. Chijiwa, T. Okamura, K. Akashi, Y. Fukumaki, Y. Niho, H. Sasaki, Expression of DNA methyltransferases DNMT1, 3A, and 3B in normal hematopoiesis and in acute and chronic myelogenous leukemia, Blood 97 (2001) 1172–1179.
[28] P.O. Esteve, H.G. Chin, S. Pradhan, Human maintenance DNA (cytosine-5)-methyltransferase and p53 modulate expression of p53-repressed promoters, Proc. Natl. Acad. Sci. USA 102 (2005) 1000–1005.
[29] T.J. Ley, L. Ding, M.J. Walter, M.D. McLellan, T. Lamprecht, D.E. Larson, C. Kandoth, J.E. Payton, J. Baty, J. Welch, C.C. Harris, C.F. Lichti, R.R. Townsend, R.S. Fulton, D.J. Dooling, D.C. Koboldt, H. Schmidt, Q. Zhang, J.R. Osborne, L. Lin, M. O'Laughlin, J.F. McMichael, K.D. Delehaunty, S.D. McGrath, L.A. Fulton, V.J. Magrini, T.L. Vickery, J. Hundal, L.L. Cook, J.J. Conyers, G.W. Swift, J.P. Reed, P.A. Alldredge, T. Wylie, J. Walker, J. Kalicki, M.A. Watson, S. Heath, W.D. Shannon, N. Varghese, R. Nagarajan, P. Westervelt, M.H. Tomasson, D.C. Link, T.A. Graubert, J.F. Dipersio, E.R. Mardis, R.K. Wilson, DNMT3A Mutations in Acute Myeloid Leukemia, N. Engl. J. Med. 363 (2010) 2424–2433.